Target-specific short-term dynamics are important for the function of synapses in an oscillatory neural network

Akira Mamiya[3], **Farzan Nadim**[1,2]

[1] Department of Mathematical Sciences and
Center for Applied Mathematics and Statistics
New Jersey Institute of Technology, Newark, NJ 07102

[2] Dept of Biological Sciences, Rutgers University-Newark

[3] Center for Molecular and Behavioral Neuroscience, Rutgers University-Newark

CAMS Report 0405-09, Fall 2004

Center for Applied Mathematics and Statistics

NJIT

Target-specific short-term dynamics are important for the function of synapses in an oscillatory neural network

Akira Mamiya

Center for Molecular and Behavioral Neuroscience, Rutgers University, Newark, NJ 07102. mamiya@cshl.edu

(Present Address: Cold Spring Harbor Laboratory, Cold Spring Harbor, NY 11742)

Farzan Nadim

Department of Mathematical Sciences, New Jersey Institute of Technology and Department of Biological Sciences, Rutgers University, Newark, NJ 07102. farzan@njit.edu

Abbreviated title: Target-specific synaptic dynamics in a neural oscillator

Corresponding Author: Farzan Nadim, Department of Biological Sciences, Rutgers University. 101 Warren St., Newark, NJ 07102, Phone (973) 353-1541, Fax (973) 353-1007, Email: farzan@njit.edu

Key words: pyloric rhythm, stomatogastric ganglion, lobster, synaptic depression, modeling

Abstract

Short-term dynamics such as facilitation and depression are present in most synapses and are often target-specific, even for synapses from the same type of neuron. We examine the dynamics and possible functions of two synapses from the same presynaptic neuron in the rhythmically active pyloric network of the spiny lobster. Using simultaneous recordings, we show that the synapses from the lateral pyloric (LP) neuron to the pyloric dilator (PD) and the pyloric constrictor (PY) neurons both show short-term depression. However, the postsynaptic potentials produced by the LP to PD synapse are larger in amplitude, depress less and recover faster than those produced by the LP to PY synapse. We show that the synapse from the LP neuron to the PD neuron, the latter a member of the pyloric pacemaker ensemble, functions to slow down the pyloric rhythm when it is fast and to speed it up when it is slow. In contrast, the synapse from the LP neuron to the PY neuron functions to delay the activity phase of the PY neuron at all cycle periods. Using a computational model of the pyloric network, we show that the short-term dynamics of synaptic depression observed for each of these synapses are tailored to their individual functions and that replacing the dynamics of either synapse with the other would disrupt these functions. Together, the experimental and modeling results suggest that the target-specific features of short-term synaptic depression are functionally important for synapses efferent from the same presynaptic neuron.

Introduction

Short-term depression is a dynamic property of many synapses (Zucker 1989). Although recent studies have proposed a variety of roles for short-term depression (Abbott et al. 1997; Chance et al. 1998; Cook et al. 2003; Galarreta and Hestrin 1998; Manor et al. 2003; Nadim et al. 2003; Reyes et al. 1998; Rose and Fortune 1999), the functional significance of this form of synaptic plasticity is still not well understood. Interestingly, synapses made by a single presynaptic neuron onto different types of target neurons can show short-term depression with different dynamics (Hunter and Milton 2001; Markram et al. 1998; Reyes et al. 1998; Watanabe et al. 2005). This differential control of short-term synaptic depression may provide a mechanism for the presynaptic neuron to selectively control the activity of its postsynaptic targets (Markram et al. 1998). However, so far no detailed study has investigated whether the differences in the short-term dynamics observed between synapses made by a single presynaptic neuron to different targets are of true functional importance.

We used the rhythmically active pyloric circuit of the spiny lobster, *Panulirus interruptus*, to explore the possible functional significance of the distinct dynamics of short-term depression in two synapses efferent from a single presynaptic neuron. In this circuit, the lateral pyloric (LP) neuron is presynaptic to multiple targets, including the pyloric dilator (PD) neurons and the pyloric constrictor (PY) neurons (Selverston et al. 1976). Both the LP to PD synapse and the LP to PY synapse are known to show short-term synaptic depression (Mamiya et al. 2003; Manor et al. 1997). Although their dynamics have not been compared in the same preparations, parameters that describe short-term depression of these synapses are very different (Mamiya et al. 2003; Manor et al. 1997). Since the PD neurons, together with the anterior burster (AB) neuron, are members of the pacemaker ensemble of the pyloric network,

whereas PY neurons are followers, the functions of these two synapses may also be different. The LP to PD synapse provides the sole chemical synaptic feedback to the pyloric pacemaker group from the follower neurons and has been shown to be important for controlling the period of the pyloric rhythm (Mamiya and Nadim 2004; Nadim et al. 1999; Weaver and Hooper 2003a). In contrast, the LP to PY synapse has been proposed to be important for controlling the burst phase of the postsynaptic PY neuron (Mamiya et al. 2003).

In this study, we characterized and directly compared the short-term synaptic dynamics of the LP to PD and the LP to PY synapses. We then tested the functional roles of these synapses by functionally removing them from the network and observing the effect on the period of the pyloric rhythm and the burst phase of the PY neurons. Finally, we developed a computational model of the pyloric circuit, incorporating the dynamics of the two LP neuron efferent synapses, and tested the hypothesis that the difference in the short-term dynamics of these two synapses are important for the function of each synapse. Using the model, we show that when the short-term dynamics of the LP to PD and the LP to PY synapses are replaced with the dynamics of the other synapse, the synapses fail to function normally.

Materials and Methods

Preparation and identification of the neurons

All experiments were performed on adult spiny lobsters *Panulirus interruptus* (Don Tomlinson Fisheries, San Diego, CA). The stomatogastric nervous system (STNS) was isolated following standard procedures (Harris-Warrick 1992; Selverston et al. 1976). The isolated STNS was pinned down on a Sylgard-coated Petri dish and superfused throughout each experiment with chilled (16°C) physiological saline containing (in mM): 479.0 NaCl; 12.9 KCl; 13.7 $CaCl_2 \bullet 2H_2O$; 10.0 $MgSO_4 \bullet 7H_2O$; 3.9 $NaSO_4 \bullet 10H_2O$; 11.2 Trizma base; 5.1 Maleic acid, pH=7.45.

Pyloric neurons were identified according to their stereotypical axonal projections in identified nerves using conventional techniques (Harris-Warrick 1992; Selverston et al. 1976). The pyloric activity was monitored extracellularly with stainless steel wire electrodes from identified nerves. Extracellular signals were amplified by a differential AC amplifier model 1700 (A-M systems, Carlsborg, WA). Intracellular recordings were made by impaling the somata with glass microelectrodes filled with 0.6 M K_2SO_4 + 20 mM KCl (for identification of neurons and intracellular recordings; resistance 30-35 MΩ) or 3M KCl (for current injection only; resistance 8-12 MΩ). All intracellular recordings were done with Axoclamp 2B amplifiers (Axon Instruments, Union City, CA).

Comparison of the short-term dynamics of the LP to PD and the LP to PY synapses

To compare the short-term dynamics of the LP to PD and the LP to PY synapses, we activated these synapses (see below) and recorded the postsynaptic potentials simultaneously from both the PD and PY neurons. For better control of the membrane voltage, synaptic potentials were measured after abolishing the pyloric

rhythm. Bath application of 0.1 μM tetrodotoxin (TTX; Biotium, CA) abolished this activity by blocking descending inputs to the stomatogastric ganglion. This also blocked action potential-mediated synaptic transmission in the ganglion. The current study focuses on graded synaptic transmission, which has been shown to be important and sufficient for generating the pyloric rhythm (Hartline and Graubard 1992; Manor et al. 1997; Raper 1979).

To activate the LP to PD and the LP to PY synapses simultaneously, the presynaptic LP neuron was voltage clamped (with two electrodes) and depolarized with 40 mV voltage steps. Postsynaptic potentials (PSPs) were recorded simultaneously from the PD neuron and the PY neuron in current clamp mode. To study the short-term dynamics of the synapse, the voltage step was repeated five times. The duration of the voltage step was fixed at 400 ms, and each activation set was composed of five voltage steps separated by the inter-pulse interval (IPI) of either 400, 800, 2000, 4000, or 8000 ms. For each IPI, the activation set was repeated five times. There was a 30 second interval between every two runs to allow for the complete recovery of the synapse. The LP neuron was held at a holding potential of –60 mV, close to its resting potential. The resting potentials of the PD neurons and the PY neurons did not change during the experiment and were in a range of –55 ± 5 mV in all experiments.

The LP to PY synapse has both an electrical and a chemical component (Mamiya et al. 2003). Since a specific blocker for the electrical coupling is not known in this system, it was not possible to measure the chemical component directly by blocking the electrical coupling. Instead, the chemical component was estimated by subtracting the electrical coupling component from the postsynaptic potential

recorded in Control conditions. For measurement of the electrical coupling component, the chemical synapse was blocked by bath application of 10 μM picrotoxin (PTX) (Marder and Paupardin-Tritsch 1978).

Effect of the LP to PD synapse on the pyloric rhythm period

The rhythm period was manipulated by injecting various amounts of current (–12 to +4 nA) into one of the pacemaker neurons (AB/PD) in a step-wise manner. At each step, the LP neuron was hyperpolarized (–10 nA current injection) to remove the LP to PD synapse. The rhythm period in the presence of the LP to PD synapse was the average period of 30 cycles immediately before hyperpolarizing the LP neuron. The average period of 30 cycles during LP hyperpolarization was used to measure the rhythm period in the absence of the LP to PD synapse. To avoid any transient effects, cycles within the first 10 seconds after hyperpolarization of the LP neuron were not used for the calculation of period.

Effect of the LP to PY synapse on the PY burst phase

The aim of this experiment was to study the effect of the LP to PY synapse on the burst phase of the PY neuron relative to the burst phase of the PD neuron at different rhythm periods. To remove the LP to PY synapse, the LP neuron was hyperpolarized (–10 nA current injection). This hyperpolarization also removes the LP to PD synapse and affects the period of the pyloric rhythm. Since the PY burst phase is known to change according to the period of the pyloric rhythm (Hooper 1997a; 1997b), direct comparison of the PY burst phase with and without the LP to PY synapse cannot distinguish whether any effect seen is due to the removal of the synapse or simply due to the change in cycle period. To separate these two factors, it was necessary to manipulate the rhythm period and compare the PY burst phase with

and without the LP to PY synapse for cycles that had the same period.

For manipulation of the rhythm period, a slowly changing ramp current was injected into one of the PD neurons. The current was changed from 0 nA to –12 nA at a rate of –0.1 nA per second, then from –12 nA to +4 nA at a rate of 0.1 nA per second, and finally from +4 nA back to 0 nA at a rate of –0.1 nA per second. This ramp current was injected both in the presence of the LP to PY synapse and when it was removed by hyperpolarizing the LP neuron. The PY burst phase was calculated for all the cycles and was grouped according to the period of the cycle using 10 ms bins. Since the hyperpolarization of the LP neuron affects the rhythm period, the range of the rhythm period observed in response to the current injection was different between the cases with and without the LP hyperpolarization. Only the bins that had more than five cycles in both cases were used for the comparison of the PY burst phase. The average burst phase of the first five cycles in each bin was used for the comparison.

Recording, Analysis, and Statistics

All intracellular recordings were digitized at 4 kHz and stored on a PC using a PCI-6070-E board (National Instruments, Austin, TX) and custom-made recording software Scope (available for download at http://stg.rutgers.edu/software) developed in the LabWindows/CVI software environment (National Instruments, Austin, TX). All analysis, such as detection of the peak amplitude of the postsynaptic response, averaging of the synaptic response, calculation of the ratios, digital subtraction of the traces, curve fitting, and calculation of the period and phase were done by custom-made programs written in Matlab (MathWorks Inc., Natick, MA). Statistical tests were done using a SAS package (SAS Institute Inc., Cary, NC).

A model of the pyloric circuit

All neurons, with the exception of the LP neuron, were modeled as conductance-based Hodgkin and Huxley (1952) type neurons. Each neuron was modeled with 2 compartments representing the axon (A) and the rest of the neuron (S/N: soma, primary and secondary neurites). This spatial arrangement was chosen to isolate the spike-generation zone (axon) from the site of synaptic inputs and slower intrinsic ionic currents (Soto-Treviño et al. 2005). All synapses connected the S/N compartments of the neurons. Our choice not to use a biophysically realistic model of the LP neuron was intentional so that we could remove any confounding effects of the AB, PD and PY synapses back to the LP neuron from our model results and focus on the significance of the LP to PD and PY synaptic dynamics. The LP neuron was instead modeled using a library of waveforms as follows. Recordings of the LP neuron membrane potential waveform were low-pass filtered at 10 Hz, normalized in amplitude and divided into individual cycles or unitary waveforms (Mamiya and Nadim 2004). These unitary waveforms were sampled at 1000 points each (with the first and last points corresponding to two consecutive burst onsets of the PD neuron), categorized according to their cycle period and averaged in 10 ms bins to build a library of LP neuron waveforms, indexed by the waveform period. The membrane potential of the model LP neuron was produced by playing back the appropriate pre-recorded waveform from the library, beginning with each burst of the PD neuron. The LP waveform chosen for each cycle was the one whose period matched the last cycle period of the PD neuron. The model LP neuron membrane potential was scaled to oscillate between –60 and –30 mV. Since the voltage of the model LP neuron was predetermined, the model LP neuron did not receive any synaptic input. There was, however, a synapse from the LP neuron to both the PD and the PY neurons. There was also a synapse from the AB neuron to the PY neuron.

All simulations were performed using Network, a home-developed software running on the Linux platform, with a 4th order Runge-Kutta integration method and dt = 0.05 ms.

Equations

In each segment of the model neurons, the membrane potential, V, was obtained by numerical integration of the differential equation

$$-C\frac{dV}{dt} = I_{leak} + \sum I_{ion} + I_{syn} + I_{axial} - I_{external}$$

where C is the membrane capacitance. Each ionic current was modeled as

$$I_{ion} = g_{ion} m^p h^q (V - E_{ion})$$

where q = 0 or 1 and m and h are governed by the equations (with x representing m or h):

$$\begin{aligned} \tau_x(V)\frac{dx}{dt} &= x_\infty(V) - x \\ x_\infty(V) &= 1/(1+e^{(V-V_k)/k}) \\ \tau_x(V) &= \tau_1 + \tau_2 x_\infty(V). \end{aligned} \qquad (1)$$

The parameter values for the AB and the PD neurons were based on the model of Soto-Treviño et al (2005) with an addition of a low threshold calcium current in the PD neuron. The parameter values for the low threshold calcium current were: $\boldsymbol{g}_{CaLo}$ = 0.02 nS, p = 2, q = 1, $m_\infty(V_m)$ = 1/(1+exp(−(V_m+60)/2)), τ_m = 25 ms, $h_\infty(V_m)$ = 1/(1+exp((V_m+67)/2)), τ_m= 100 + 500 $h_\infty(V_m)$.

The parameter values for the ionic and leak currents in the PY neuron are given in Table 1.

The synaptic currents were computed using

$$I_{syn} = g_{syn} ad(V_{post} - E_{syn})$$

where a represented the activation of the synapse and d represented synaptic depression (Bose et al. 2001; Manor et al. 2003). The variables a and d were also governed by Equation (1), with x representing a or d. All the synapses connected the S/N compartments of the model neurons. The parameter values for the synaptic currents are given in Table 2.

Results

In the pyloric circuit of the spiny lobster, *Panulirus interruptus*, the LP neuron is presynaptic to several targets, including the PD neurons and the PY neurons (Fig. 1 inset) and oscillates out of phase with both neurons during an ongoing pyloric rhythm (Fig. 1). We characterized and compared the dynamics and the function of the synapses from the LP neuron to the PD and PY neurons. The study was done in three steps. First, we compared the short-term dynamics of the LP to PD synapse with those of the LP to PY synapse. Second, we confirmed and quantified the functional effects of these synapses by removing them during the ongoing pyloric rhythm and observing the change in the properties of the pyloric rhythm. Finally, we made a computational model of a reduced pyloric circuit to test the hypothesis that the short-term dynamics observed for each synapse in the first step are essential for the function of the synapse observed in the second step. Together, the results suggest that the short-term dynamics of the synapse are differentially regulated to suit the specific function of the synapse.

Comparison of the dynamics of the LP to PD synapse with those of the LP to PY synapse

As a first step in understanding the relationship between the short-term dynamics of a synapse and the function of that synapse, we compared the short-term dynamics of two synapses from the same neuron to different targets. Our hypothesis was that, if the short-term synaptic dynamics are important for the function of the synapse, these two functionally distinct synapses should have different dynamics despite the fact that they originate from the same presynaptic neuron.

To study the dynamics of the LP to PD and the LP to PY synapses, we voltage clamped the LP neuron and activated the synapses with a train of five voltage pulses (amplitude 40 mV, duration 400 ms) with different interpulse intervals (IPIs: 400, 800,

2000, 4000, and 8000 ms). Figure 2A shows an example of voltage traces from the LP, PD, and PY neurons when these synapses were activated with an IPI of 400 ms. The PSPs in the PD and PY neurons showed very different dynamics (Fig. 2A; second and third trace). In the PD neuron, the amplitude of the PSP depressed approximately 40% from the first pulse to the second pulse. Most of the depression took place between the first and the second pulse, and the response stabilized as a hyperpolarizing response. On the other hand, the simultaneously recorded PSPs in the PY neuron switched from hyperpolarizing to depolarizing in the middle of the first pulse. The PSP in response to the second pulse was completely depolarizing and the response stabilized as a depolarizing response.

The switch from a hyperpolarizing to a depolarizing response in the PY neuron was caused by an interaction between the two components of this synapse: a depressing chemical component and non-depressing electrical coupling component (Mamiya et al. 2003). Since there is no known specific blocker for electrical coupling in this system, we approximated the amplitude of the chemical component by blocking the chemical component (by bath application of 10^{-5} M PTX) and subtracting the remaining (purely electrical) PSP (Fig. 2A; PY_{ptx}) from the control trace (Fig. 2A; PY_{ctl}). After subtracting the electrical coupling component, we found a highly depressing chemical synapse (Fig. 2A; $PY_{ctl-ptx}$). The amplitude of the chemical synapse depressed more than 90% by the second pulse.

To compare the extent of depression and the rate of recovery of the LP to PD and the LP to PY (chemical component) synapses, we used the conventional paired-pulse recovery paradigm. For each synapse, the paired-pulse recovery ratio was calculated for each IPI by taking the ratio of the peak amplitude in response to

the 2nd pulse (A_2) to that in response to the 1st pulse (A_1; see inset of Fig. 2B). This is a value between 0 and 1, showing how much the synapse has recovered during the IPI (1 = complete recovery). Figure 2B shows the average paired-pulse recovery ratios of the LP to PD and the LP to PY synapses for five different IPIs (mean±SD, N=5). As seen in the figure, the LP to PD synapse had a greater recovery ratio than the LP to PY synapse for all IPIs, but the difference between the two recovery ratios was larger when the interval was short. To quantify the extent of synaptic depression and the time course of the recovery, we fit the relationship between the paired pulse recovery ratio and the IPI with a single exponential decay function $1 - D_{max} \exp(-IPI/\tau_{rec})$, where τ_{rec} is the time constant of recovery and D_{max} is the amount of depression when the IPI tends to zero. The y-intercept of this exponential function ($R_0 = 1 - D_{max}$, indicated by an arrow in Fig. 2B) shows the extent of recovery as the IPI tends to 0. For the example shown in Fig. 2B, the LP to PD synapse had smaller τ_{rec} and D_{max} than the LP to PY synapse (τ_{rec} = 2.80 s compared to 4.38 s, D_{max} = 0.456 compared to 0.916), reflecting the fact that the LP to PD synapse depressed less and recovered faster than the LP to PY synapse.

A scatter plot of τ_{rec} versus D_{max} for 8 paired recording of LP to PD and LP to PY synapses (Fig. 2C) shows two clearly separated clusters, corresponding to two synapses. In all cases, the LP to PD synapse had significantly smaller τ_{rec} and D_{max} values than the simultaneously recorded LP to PY synapse (Student's *t*-test, $p < 0.05$ and $p < 0.001$ for τ_{rec} and D_{max} respectively, N=8). These results indicate that the LP to PD synapse always depressed less and recovered faster than the LP to PY synapse. Moreover, a comparison between the amplitude of the chemical synapse in response to the first pulse (A_1) showed that A_1 was significantly larger in the LP to PD synapse than in the LP to PY synapse (-8.80 ± 6.44 mV compared to -2.12 ± 0.55 mV; mean ±

SD; Student's *t*-test, p = 0.00014, N= 8; data not shown).

Quantifying the effect of the LP to PD synapse on the period of the pyloric rhythm and the effect of the LP to PY synapse on the phase of the PY burst.

To examine the relationship between the short-term dynamics of the synapse and the function of that synapse, we contrasted and quantified the previously proposed functions of the LP synapses to the PD and PY neurons. For the LP to PD synapse, we investigated its effect on the period of the pyloric rhythm (Mamiya and Nadim 2004; Weaver and Hooper 2003a, b). For the LP to PY synapse, we investigated its effect on the phase of the PY burst (Mamiya et al. 2003). Both effects were studied while manipulating the rhythm period to quantify how the change in the rhythm period affects the function of the synapses.

The effect of the LP to PD synapse on the period of the pyloric rhythm

To investigate the effect of the LP to PD synapse on the period of the pyloric rhythm, we removed the synapse during the ongoing rhythm (see Methods) and compared the PD neuron cycle period in the presence and absence of the synapse (Fig. 3A). In a previous study, we proposed that the LP to PD synapse acts to lengthen the rhythm period when the period is short while it acts to shorten the period when it is long (Mamiya and Nadim 2004). To test this hypothesis, we manipulated the rhythm period (see Methods) and investigated the effect of the removal of the LP to PD synapse at different rhythm periods. We calculated the average rhythm period in the presence ($Period_{withLP}$) and absence ($Period_{withoutLP}$) of the LP to PD synapse at different cycle periods. The parameter ΔPeriod (= $Period_{withLP} - Period_{withoutLP}$) shows the change in the rhythm period due to the actions of the LP to PD synapse. The change observed was consistent with our hypothesis: a scatter plot of the ΔPeriod

versus the $Period_{withoutLP}$ (Fig. 3B; N=13 preparations) shows that the LP to PD synapse significantly increased the rhythm period when the period was short but decreased it when it was long (Fig. 3B, the best linear fit line $\Delta Period = 86.3 – 0.0900 \times Period_{withoutLP}$ showed a negative correlation $r = -0.343$, $p = 0.0073$).

Although the negative correlation between $\Delta Period$ and $Period_{withoutLP}$ was statistically significant overall, the correlation was weak and the $\Delta Period$ varied greatly even for the same $Period_{withoutLP}$. A previous study has shown that the hyperpolarization of the LP neuron changes the activity of another neuron (the ventral dilator VD) in some but not all preparations, presumably through the removal of the inhibitory LP to VD synapse (Weaver and Hooper 2003b). It is also known that the VD neuron affects the rhythm period through a rectifying electrical coupling between the VD and PD neurons (Weaver and Hooper 2003a). Thus, we suspected that hyperpolarization of the LP neuron might also have an indirect effect on the rhythm period through its effect on the activity of the VD neuron, and that this effect might vary across preparations. To test whether this indirect effect was the cause of the variability seen in the $\Delta Period$ data, we repeated the above experiment in a subset of preparations (N=4 out of 13) before and after hyperpolarizing the VD neuron, and compared the relationship between the $\Delta Period$ and the $Period_{withoutLP}$ in the two cases. Hyperpolarization of the VD neuron should remove its effect on the pyloric rhythm period by removing the positive current flow from the VD neuron to the PD neuron. These 4 preparations alone did not show a statistically significant negative correlation (gray circles in Fig. 3B; $r = -0.329$, $p = 0.15$ for these 4 preparations). However, when the effect of the VD neuron was removed in these preparations, the negative correlation between $\Delta Period$ and $Period_{withoutLP}$ became stronger and statistically significant (Fig. 3C, $r = -0.543$, $p = 0.013$; best linear fit line $\Delta Period = 88.5 – 0.0948$

$\times$ $Period_{withoutLP}$). This result indicates that some variability in the data is due to the difference in the indirect effect, through the VD neuron, of removing the LP neuron on the pyloric period.

The effect of the LP to PY synapse on the burst phase of the PY neuron

A previous study has suggested that the LP to PY synapse may help maintain the burst phase of the PY neuron constant over a wide range of rhythm frequencies (Mamiya et al. 2003). To examine the effect of the LP to PY synapse on the burst phase of the PY neuron (relative to the PD neuron burst onset), we removed the LP to PY synapse during the ongoing rhythm (see Methods) and compared the burst phase in the presence and absence of the synapse (Fig. 4A).

Because hyperpolarization of the LP neuron changes the rhythm period through the removal of the LP to PD synapse, we also varied the rhythm period (see Methods) and compared the PY burst phase in the two cases between cycles that had the same period. This allowed us to separate the effect of the LP to PY synapse from the effect of cycle period on the burst phase of the PY neuron. A scatter plot of the average PY burst phase with and without the LP to PY synapse versus the rhythm period shows that the LP to PY synapse acted to delay the PY burst phase (Fig.4B; Student's t-test, $p = 0.00001$, N=12 PY neurons).

The effect of the rhythm period on the burst phase of the PY neuron can be measured more clearly by calculating the difference between the PY burst phase in the presence and absence of the LP to PY synapse ($\Delta Phase = Burst\ Phase_{withLP} - Burst\ Phase_{withoutLP}$). A scatter plot of $\Delta Phase$ versus the rhythm period shows mostly positive values of $\Delta Phase$ (Fig. 4C). However, there was no significant correlation

between ΔPhase and the rhythm period (Fig. 4C, r = −0.0649, p = 0.235). Nonetheless, the scatter plot shows that there are two groups of ΔPhase values, one that does not change with the period, and another that increases with the period (gray circles in Fig. 3C). Post-hoc analysis of the relationship between the ΔPhase and the rhythm period for individual PY neurons showed that in 3 out of 12 neurons, the ΔPhase value showed a significant positive correlation with the period ($p < 0.05$; the Dunn-Sidak corrected value of 4.26×10^{-3} was used to account for the multiple comparisons). A scatter plot of the ΔPhase versus the rhythm period for these 3 neurons only shows that there was a significant positive correlation between these two parameters for these neurons (Fig. 4D; r = 0.683, p = 0.0001; best linear fit line $\Delta\text{Phase} = -0.15 + 3.42 \times 10^{-4} \times \text{Period}$). These results show that the LP to PY synapse acts to delay the burst onset of some PY neurons if the cycle period becomes longer and thus helps maintain a constant PY burst phase.

The computational model of the LP to PD and LP to PY synaptic dynamics

In order to investigate the function of the short-term dynamics observed in the LP to PD and LP to PY synapses, we used a computational model of the pyloric network and incorporated the experimentally measured synaptic dynamics. The computational model included a pacemaker group consisting of AB and PD neurons, coupled electrically to oscillate in phase (Soto-Treviño et al. 2005). The AB neuron had an inhibitory synapse to the follower PY neuron, causing the PY neuron to oscillate out of phase with the AB and PD neurons (Fig. 5B). The intention of this computational study was not to produce the correct phasing of the LP neuron, but rather to see the effect of the efferent LP synapses on the PD and PY neurons. Thus, instead of using a biophysically realistic model of the LP neuron, we used an extensive library of LP neuron waveforms (Mamiya and Nadim 2004) to model the

membrane potential oscillation of the LP neuron (see Methods). The LP to PD and LP to PY synapses were computed using these membrane potential oscillations as the presynaptic input. By using the pre-recorded library of LP neurons, we were able to activate the LP to PD and LP to PY synapses at the correct phase of oscillation, depending on the oscillation period, and thus we not only removed a degree of complexity from the model, but also retained relatively accurate presynaptic membrane potentials for the synapses of interest.

The synapse from the AB neuron to the PY neuron had both a depressing and a non-depressing component, matching preliminary recordings from our laboratory (data not shown), and was tuned empirically to produce the correct activity phase in the PY neurons. The dynamics of the LP to PD and LP to PY synapses were matched to the dynamics shown in Figure 2. The model also included a previously characterized rectifying electrical coupling between the LP and PY neurons that allowed positive current to flow from the LP neuron to the PY neuron (Mamiya et al. 2003). Figure 5A shows the postsynaptic potentials in the model PD and PY neurons in response to a train of 40 mV voltage pulses applied to the voltage clamped model LP neuron. Also shown are the PSPs in the PY neuron without the chemical component (PY_{ptx}) or the electrical component ($PY_{ctl\ -ptx}$) for comparison with the biological traces shown in Figure 2A.

The effect of the LP to PD synapse on the oscillation period in the computational model

To examine the effect of the LP neuron on the period of the AB and PD neurons, we changed the model cycle period by current injection into the AB neuron and measured the influence of the LP to PD synapse on the period by setting the

maximal synaptic conductance to 0 and thus eliminating the synapse (Fig 6A). We then compared the difference between the periods with and without the LP to PD synapse ($\Delta Period = Period_{withLP} - Period_{withoutLP}$) at different baseline periods ($Period_{withoutLP}$). Consistent with the experimental results presented in Figure 3, at fast oscillation periods, the LP to PD synapse acted to slow down the rhythm, whereas at slow periods it sped up the rhythm (Fig. 6B, Control: filled circles). Although these results were not quantitatively the same as the experimental results, they do match qualitatively. By changing the various ionic conductances in the model PD and AB neurons, we found that the effect of the LP to PD synapse to speed up a slow oscillation period was mainly due to the influence of the synapse on a low-threshold Ca^{++} current. At slower cycle periods, the LP to PD inhibition became larger in amplitude due to recovery from depression. This larger inhibition of the PD neuron allowed more recovery from inactivation of the low-threshold Ca^{++} current, causing the PD neuron to burst earlier. In contrast, there was little change in the hyperpolarization-activated inward current I_h, possibly because its activation kinetics was too slow to have different effects at different cycle periods. However, incorporating additional low-threshold potassium (A) current in the AB or PD model neurons also counteracted the ability of the LP to PD synapse to speed up the rhythm when it was slow (data not shown).

To understand the functional significance of the dynamics of the LP to PD synapse, we replaced the equations governing these dynamics with those governing the dynamics of the chemical LP to PY synapse. We then tuned the maximum conductance of this surrogate synapse so that, at the highest current injection value into the AB neuron, the oscillation period matched that of the control synapse (leftmost points in Fig. 6B). In contrast to the control synapse, the surrogate synapse

acted to slow down the rhythm at all periods (Fig. 6B, empty squares). Similarly, when the maximal conductance of the surrogate synapse was tuned to match the oscillation with the control synapse at the longest period, it acted only to speed up the rhythm at high periods but would disrupt the rhythm at low periods (data not shown).

The effect of the LP to PY synapse on the phase of the PY neuron in the computational model

The experiments described in Figure 4 show that the LP to PY synapse acts to delay the phase of the PY neuron activity at all oscillation periods. We tested this effect in the computational model by comparing the phase of the PY neuron activity in control conditions and when the LP to PY maximal synaptic conductance was set to 0 (Fig. 7A). These results are summarized in Fig. 7B, showing that the model synapse delayed the PY activity phase by 0.11 to 0.17 at different cycle periods. Although these results do not quantitatively match the experiments, they do qualitatively (compare Fig. 4B).

To test the effect of synaptic dynamics on the activity phase of the PY neurons, we replaced the equations governing the dynamics of the LP to PY synapse so that its chemical component followed the dynamics of the LP to PD synapse. We then tuned the maximum conductance of the surrogate LP to PY synapse so that the activity phase of the PY neuron matched the phase with the control synapse at the fastest cycle period (Fig. 7A, right panel, compare 3rd and 5th traces). When the cycle period was increased by reducing external current injected into the AB neuron, the surrogate LP to PY synapse did not allow the PY neuron to produce action potentials and the PY neuron only displayed subthreshold activity (Fig. 7A, left panel, compare 3rd and 5th traces). Similarly, if the maximal conductance of the surrogate LP to PY synapse

was tuned to match the PY phase of the control synapse at any single period, increasing the period caused a suppression of action potentials (data not shown).

Discussion

We examined the hypothesis that, in a distributed network, the short-term dynamics of synapses are important for the proper function of the neuronal network. If this is indeed the case, these dynamics should be controlled to match the function of the respective synapse. In particular, differential control of short-term synaptic depression might allow the presynaptic neuron to differentially control the activity of different postsynaptic neurons (Markram et al. 1998; Reyes et al. 1998). Thus, we examined the possible functional significance of the differential control of short-term synaptic depression of separate synapses efferent from the same presynaptic neuron. By comparing two functionally different synapses in the lobster pyloric circuit, we first showed that these synapses exhibit short-term depression with different dynamics and second, that this difference in dynamics may be important for the proper operation and function of each synapse.

The LP to PD synapse depresses less and recovers faster than the LP to PY synapse

Previous studies on short-term depression of the LP to PD synapse (Manor et al. 1997) and the LP to PY synapse (Mamiya et al. 2003) have indicated that these synapses might have different dynamics. However, since the protocols for the activation of the synapses were different in each of these previous studies, a direct comparison of the dynamics was not feasible. In the present study, we directly compared these two synapses in the same preparations and showed that they have different strengths and dynamics. In particular, the LP to PD synapse was stronger, depressed less and recovered faster than the LP to PY synapse (Fig. 2C).

Although, there was a clear difference between the dynamics of the short-term depression of the LP to PD and the LP to PY synapses, there was also some variability in dynamics even within the same type of synapse. In a previous study, we showed that

the variability in the short-term depression of the LP to PY synapse was correlated with the burst phase of the PY neuron (Mamiya et al. 2003). Therefore, the variability in the short-term depression of the LP to PY synapse observed in this study probably reflected the differences in the firing phase of the 6-8 postsynaptic PY neurons. However, no previous study has examined the variability in the short-term depression of the LP to PD synapse. Since the LP to PD synapse had been proposed to play an important role in controlling the period of the pyloric rhythm, we examined the possible correlations between the parameters that describe the short-term depression of the LP to PD synapse (maximum depression and time constant of recovery) and the period of the ongoing pyloric rhythm. However, we saw no correlations between these parameters (data not shown). Thus, the reasons for the variability in the parameters of short-term depression of the LP to PD synapse remain unknown.

Effect of the LP to PD synapse on the period of the pyloric rhythm

There have been conflicting reports on the effect of the LP to PD synapse on the period of the pyloric rhythm (Mamiya and Nadim 2004; Weaver and Hooper 2003a). Despite using similar experimental protocols, one study concluded that the LP to PD synapse increases the period of the pyloric rhythm by a constant amount regardless of the rhythm period (Weaver and Hooper 2003a), while the other study (from our laboratory) suggested that the effect of the LP to PD synapse on the period of the rhythm changes with the rhythm period (Mamiya and Nadim 2004). The results from this study are consistent with the latter study, showing that the LP to PD synapse increased the period of the rhythm when the period was short, but decreased it rhythm when the period was long. One possible reason for the discrepancy between these two studies is the difference in the method of analysis used. We chose to average the data across different preparations and took advantage of the large sample size when

performing statistical analysis. On the other hand, Weaver and Hooper (2003a) analyzed their data one preparation at a time and used a conservative way to calculate the difference between the period with and without the LP to PD synapse. In their method of analysis, the cycle periods collected with and without the LP to PD synapse were plotted together with both a series with the LP to PD synapse in descending order and a series without the LP to PD synapse in ascending order. Since the effect of the LP to PD synapse is highly variable (especially when the VD neuron, another member of the pyloric network, is not removed) this conservative way of analysis may have failed to detect the change in the effect of the LP to PD synapse at different periods of the pyloric rhythm.

Effect of the LP to PY synapse on the burst phase of the PY neuron

The LP to PY synapse consistently delayed the burst phase of the PY neuron. This may seem surprising since the activation of the synapse with a train of voltage pulses showed that, after the first pulse, the postsynaptic potential is mostly depolarizing (see Fig. 2 and Mamiya et al (2003)}. How could a depolarizing synapse delay the burst onset of the postsynaptic neuron? The reason for this paradoxical effect of the LP to PY synapse seems to be that the PSPs were measured when the pyloric activity was blocked and the PY neurons were quiescent at their resting potential of around –55 mV. However, during an ongoing pyloric rhythm, the PY neurons oscillate at much more depolarized potentials (see Fig. 1B for example). When the PY neuron is at a more depolarized potential, the driving force for the chemical inhibition component of the synapse increases while the driving force for the (rectifying) electrical coupling component decreases. Moreover, in a previous study, we showed that the LP to PY synapse depresses less when the synapse is activated with a realistic presynaptic waveform (Mamiya et al. 2003). Thus, during an

ongoing rhythm, the LP to PY synapse may in fact act to hyperpolarize the PY neuron and thus delay the onset of its burst. This is in fact exactly what happens in our computational model of the pyloric circuit in which the total LP to PY synaptic current remains outward during the ongoing rhythm (not shown).

In the pyloric circuit, the tri-phasic pattern of activity composed of bursting by the AB/PD neurons, the LP neuron, and the PY neurons is maintained relatively constant over a wide range of frequencies (around 0.5 to 2.5 Hz) (Hooper 1997a; 1997b). Both the intrinsic properties (Hooper 1998) and synaptic properties (Manor et al. 2003; Nadim et al. 2003) of the pyloric neurons have been proposed to play a role in this phase maintenance. If the short-term depression of the LP to PY synapse is helping the PY neuron to burst at a constant phase, the synapse should delay the PY burst phase more when the period of the pyloric rhythm is longer. The results from the present study show that in some cases, the LP to PY synapse did show this type of increase in the delaying effect, while in other cases it did not. The burst phase of the PY neuron is known to be influenced by factors other than the LP to PY synapse, including synaptic inputs from the pacemaker neurons (Eisen and Marder 1984) and intrinsic properties of the PY neurons (Hartline 1979; Hooper 1998). It is possible that the variability in the effect of the LP to PY synapse on the relationship between the PY burst phase and the rhythm period is due to the preparation-dependent interaction of this synapse with these other factors. Further experiments are needed to explore the possible role of the LP to PY synapse in maintaining the burst phase of the postsynaptic PY neurons.

Target specific control of the short-term synaptic depression to suit the function of the synapse

We used computational modeling to demonstrate expressly that target-specific regulation of short-term synaptic depression contributes to the differential control of the target neurons by the LP neuron. Thus, we assayed the effect of the efferent synapses of the LP neuron and their dynamics on the synaptic targets. To this end, we used a biophysically accurate model of the pyloric pacemaker AB and PD neurons (Soto-Treviño et al. 2005) to examine the effect of the LP to PD synapse on the pyloric rhythm period, and we used a simplified model of the PY neurons that produced activity at the correct phase of the pyloric cycle and fit the dynamics of the LP to PD and LP to PY synapses to our experimental data. We represented the LP neuron in the model with a library of pre-recorded LP neuron waveforms that were indexed by their period (Mamiya and Nadim 2004): each model pyloric cycle used the LP neuron waveform indexed by the previous cycle period. Our choice not to use a biophysically realistic model of the LP neuron was intentional so that we could remove any confounding effects of the AB, PD and PY synapses back to the LP neuron from our model results and focus on the significance of the LP to PD and PY synaptic dynamics. Thus, our network model is by no means intended as an accurate representation of the pyloric network and is only intended to examine the consequences of the LP neuron synaptic dynamics.

When the dynamics of short-term depression for the LP to PD synapse were replaced with those for the LP to PY synapse in the model and the strength of the "surrogate" synapse was increased to produce the appropriate effect at the fastest period (550 ms), the LP to PD synapse failed to perform its proper function. This was mainly due to the fact that the LP to PY synapse showed much more depression and thus when the maximal conductance of the surrogate synapse was made large enough to produce the appropriate effect (ΔPeriod > 0) at fast oscillation periods (when the

synapse was most depressed), at long cycle periods (when the synapse recovered from depression) it became too strong to produce the appropriate effect (ΔPeriod < 0).

Similarly, the LP to PY model synapse also failed to perform its proper function when its dynamics were replaced with those for the LP to PD synapse. In this case, the surrogate synapse was too limited in its range of efficacy to allow the PY neuron to produce action potentials at all cycle periods (note the range of synaptic efficacies as a function of the interpulse interval in Fig. 2B). When the maximal conductance of the model surrogate synapse was tuned to match the correct PY neuron phase at any single period, the PY neuron failed to produce action potentials at other periods.

We conclude, therefore, that it is unlikely that the difference in the dynamics of short-term depression in these two synapses is just a secondary effect of other synaptic properties. Rather, these modeling results suggest that the short-term depression of each synapse is differentially controlled to precisely match the function of the synapse.

Conclusion

Controlling the dynamics of synapses efferent from the same presynaptic neuron to different types of targets may be one way of achieving flexible control in networks where each neuron synapses onto multiple targets (Markram et al. 1998; Reyes et al. 1998). However, network activity is the result of the interaction between synaptic and intrinsic membrane properties of all its elements (Clemens and Katz 2001; Katz and Frost 1996; Marder and Calabrese 1996; Nässel 2000; Ramirez and Richter 1996). An accurate comprehension of how outputs of distributed networks are

generated would require not only an understanding of the dynamics of the constituent neurons and synapses, but also an adequate matching of the synaptic dynamics to their specific targets.

Acknowledgements

We thank Pascale Rabbah and Isabel Soffer for helpful discussions and their comments on this paper.

Grants

This research was supported by National Institute of Mental Health Grant MH60605 (FN).

References

Abbott LF, Varela JA, Sen K, and Nelson SB. Synaptic depression and cortical gain control. *Science* 275: 220-224, 1997.

Bose A, Manor Y, and Nadim F. Bistable oscillations arising from synaptic depression. *SIAM J App Math* 62: 706-727, 2001.

Chance FS, Nelson SB, and Abbott LF. Synaptic depression and the temporal response characteristics of V1 cells. *J Neurosci* 18: 4785-4799, 1998.

Clemens S and Katz PS. Identified serotonergic neurons in the Tritonia swim CPG activate both ionotropic and metabotropic receptors. *J Neurophysiol* 85: 476-479, 2001.

Cook DL, Schwindt PC, Grande LA, and Spain WJ. Synaptic depression in the localization of sound. *Nature* 421: 66-70, 2003.

Eisen JS and Marder E. A mechanism for production of phase shifts in a pattern generator. *J Neurophysiol* 51: 1375-1393, 1984.

Galarreta M and Hestrin S. Frequency-dependent synaptic depression and the balance of excitation and inhibition in the neocortex. *Nat Neurosci* 1: 587-594, 1998.

Harris-Warrick RM. *Dynamic biological networks : the stomatogastric nervous system*. Cambridge, Mass.: MIT Press, 1992.

Hartline DK. Pattern generation in the lobster (Panulirus) stomatogastric ganglion. II. Pyloric network simulation. *Biol Cybern* 33: 223-236, 1979.

Hartline DK and Graubard K. Cellular and synaptic properties in the crustacean stomatogastric nervous system. In: *Dymanic Biological Networks: The Stomatogastric Nervous System*, edited by Harris-Warrick RM, Marder E, Selverston AI and Moulins M. Cambridge, MA: MIT Press, 1992, p. 31-86.

Hodgkin AL and Huxley AF. A quantitative description of membrane current and its application to conduction and excitation in nerve. *J Physiol* 117: 500-544, 1952.

Hooper SL. Phase maintenance in the pyloric pattern of the lobster (Panulirus interruptus) stomatogastric ganglion. *J Comput Neurosci* 4: 191-205, 1997a.

Hooper SL. The pyloric pattern of the lobster (Panulirus interruptus) stomatogastric ganglion comprises two phase-maintaining subsets. *J Comput Neurosci* 4: 207-219, 1997b.

Hooper SL. Transduction of temporal patterns by single neurons. *Nat Neurosci* 1: 720-726, 1998.

Hunter JD and Milton JG. Synaptic heterogeneity and stimulus-induced modulation of depression in central synapses. *J Neurosci* 21: 5781-5793, 2001.

Katz PS and Frost WN. Intrinsic neuromodulation: altering neuronal circuits from within. *Trends Neurosci* 19: 54-61, 1996.

Mamiya A, Manor Y, and Nadim F. Short-term dynamics of a mixed chemical and electrical synapse in a rhythmic network. *J Neurosci* 23: 9557-9564, 2003.

Mamiya A and Nadim F. Dynamic interaction of oscillatory neurons coupled with reciprocally inhibitory synapses acts to stabilize the rhythm period. *J Neurosci* 24: 5140-5150, 2004.

Manor Y, Bose A, Booth V, and Nadim F. The contribution of synaptic depression to phase maintenance in a model rhythmic network. *J Neurophysiol*, 2003.

Manor Y, Nadim F, Abbott LF, and Marder E. Temporal dynamics of graded synaptic transmission in the lobster stomatogastric ganglion. *J Neurosci* 17: 5610-5621, 1997.

Marder E and Calabrese RL. Principles of rhythmic motor pattern generation. *Physiol Rev* 76: 687-717, 1996.

Marder E and Paupardin-Tritsch D. The pharmacological properties of some crustacean neuronal acetylcholine, gamma-aminobutyric acid, and L-glutamate responses. *J Physiol* 280: 213-236, 1978.

Markram H, Wang Y, and Tsodyks M. Differential signaling via the same axon of neocortical pyramidal neurons. *Proc Natl Acad Sci U S A* 95: 5323-5328, 1998.

Nadim F, Booth V, Bose A, and Manor Y. Short-term synaptic dynamics promote phase maintenance in multiphasic rhythms. *Neurocomputing* 52-54: 79-87, 2003.

Nadim F, Manor Y, Kopell N, and Marder E. Synaptic depression creates a switch that controls the frequency of an oscillatory circuit. *Proc Natl Acad Sci U S A* 96: 8206-8211, 1999.

Nässel DR. Functional roles of neuropeptides in the insect central nervous system. *Naturwissenschaften* 87: 439-449, 2000.

Ramirez J-M and Richter DW. The neuronal mechanisms of respiratory rhythm generation. *Curr Opin Neurobiol* 6: 817-825, 1996.

Raper JA. Nonimpulse-mediated synaptic transmission during the generation of a cyclic motor program. *Science* 205: 304-306, 1979.

Reyes A, Lujan R, Rozov A, Burnashev N, Somogyi P, and Sakmann B. Target-cell-specific facilitation and depression in neocortical circuits. *Nat Neurosci* 1: 279-285, 1998.

Rose GJ and Fortune ES. Frequency-dependent PSP depression contributes to low-pass temporal filtering in Eigenmannia. *J Neurosci* 19: 7629-7639, 1999.

Selverston AI, Russell DF, and Miller JP. The stomatogastric nervous system: structure and function of a small neural network. *Prog Neurobiol* 7: 215-290, 1976.

Soto-Treviño C, Rabbah PM, Marder E, and Nadim F. A computational model of electrically coupled, intrinsically distinct pacemaker neurons. *Submitted to J Neurophys*, 2005.

Watanabe J, Rozov A, and Wollmuth LP. Target-Specific Regulation of Synaptic Amplitudes in the Neocortex. *J Neurosci* 25: 1024-1033, 2005.

Weaver AL and Hooper SL. Follower neurons in lobster (Panulirus interruptus)

pyloric network regulate pacemaker period in complementary ways. *J Neurophysiol* 89: 1327-1338, 2003a.

Weaver AL and Hooper SL. Relating Network Synaptic Connectivity and Network Activity in the Lobster (Panulirus interruptus) Pyloric Network. *J Neurophysiol*, 2003b.

Zucker RS. Short-term synaptic plasticity. *Annu Rev Neurosci* 12: 13-31, 1989.

Tables

Table 1. PY neuron model							
Cell		**Curr.**	**g_{ion} (nS)**	**E_{ion} (mV)**	**State**	**x_∞**	**τ_x (ms)**
PY	A	Na^+	500	50	m^3	1/(1+exp(-0.08*(x+26)))	instantaneous
					h	1/(1+exp(0.13*(x+36)))	1+5/(1+exp(-0.13*(x+36)))
		K^+	200	-80	m^4	1/(1+exp(-0.2*(x+22)))	1+12/(1+exp(0.2*(x+22)))
		leak	0.5	-52	-		
		C_m = 25 pF, g_{axial} = 8 nS					
	S/N	K^+	12	-80	m^2	1/(1+exp(-(x+63)/5))	5
					h	1/(1+exp((x+65)/3))	200
		H	2	-10	m	1/(1+exp((x+65)/5))	450+250/(1+exp((x+65)/5))
		leak	5	-52	-		
		C_m = 250 pF, g_{axial} = 70 nS					

Table 2. Model synapses						
Synapse	**Type**	**g_{ion} (nS)**	**E_{syn} (mV)**	**State**	**x_∞**	**τ_x (ms)**
LP to PD	Depress.	0.01	-80	a	1/(1+exp(-(v+39)/5))	50+25/(1+exp((v+39)/5))
				d	1/(1+exp((v+39)/5))	400+500/(1+exp((v+39)/5))
	Non-dep	0.005	-80	a	1/(1+exp(-(v+39)/5))	25
LP to PY	Depress.	2	-80	a	1/(1+exp(-(v+39)/5))	25
				d	1/(1+exp((v+39)/5))	200+2000/(1+exp((v+39)/5))
	Gap-j.	0.5	-	Instantaneous, rectifying from LP to PY.		
AB to PY	Depress.	2	-80	a	1/(1+exp(-(v+42)))	15+100/(1+exp(v+42))
				d	1/(1+exp((v+45)/5))	200+500/(1+exp((v+45)/5))
	Non-dep	5	-80	a	1/(1+exp(-(v+42)))	15+100/(1+exp(v+42))
AB to PD	Gap-j.	0.0375	-	Instantaneous, non-rectifying		

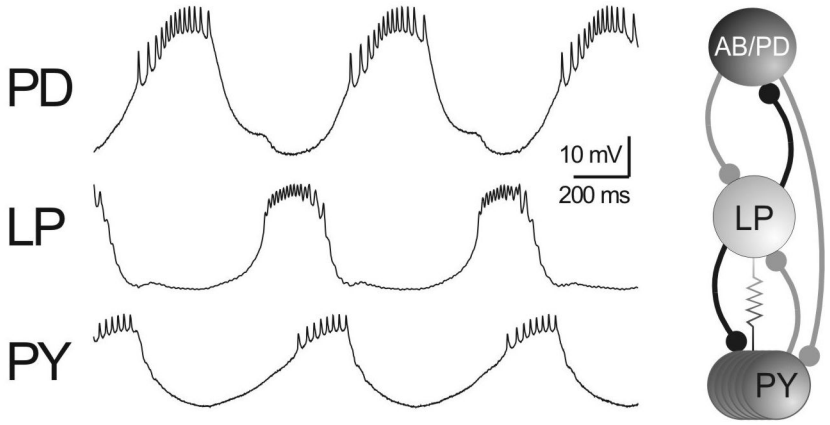

Figure 1. *The LP neuron is presynaptic to the PD and PY neurons.* Intracellular voltage traces from the PD, LP, and PY neurons show the LP neuron oscillating out of phase with both PD and PY neurons. Large IPSPs due to the LP to PD synapse can be seen in the trace for the PD neuron. The PSPs due to the LP to PY synapse are small and difficult to see during the ongoing rhythm. *Inset:* Circuit diagram shows the connectivity among the AB/PD, LP and PY neurons. The AB/PD and LP neurons are connected by reciprocally inhibitory synapses. The LP to PY synapse is a mixed electrical/chemical synapse. Minimum membrane potential values (in mV), PD: -65, LP: -58, PY: -56.

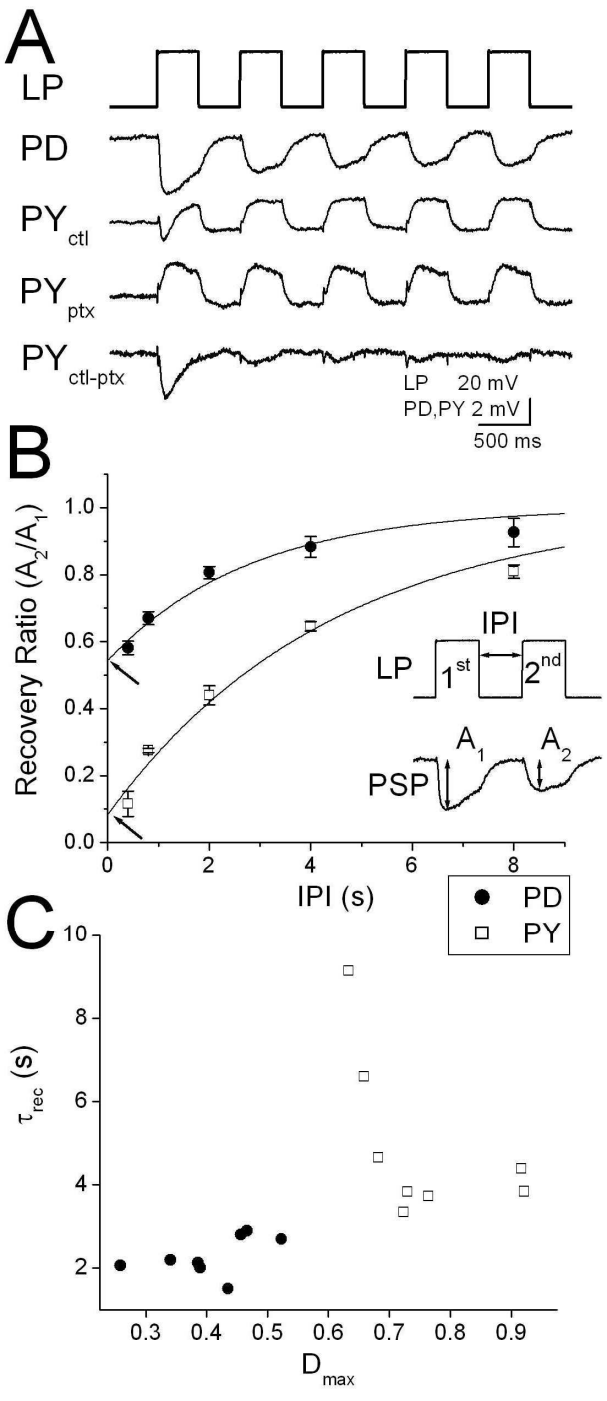

Figure 2. *The LP to PD and LP to PY synapses have different short-term dynamics.* **A**. An example of the PSPs in the PD and PY neurons in response to a train of five 40 mV voltage pulses in the LP neuron. The ptx trace shows the PSP in the PY neuron when the chemical component of the LP to PY synapse was blocked with 10 μM picrotoxin. ctl-ptx trace (bottom) shows the chemical component of the LP to PY synapse, estimated by subtracting the ptx trace from the ctl trace. **B.** The exponential fit of the paired-pulse recovery rate versus the interpulse interval (IPI) for the LP to PD and the LP to PY (ctl-ptx) synapses shown in A (mean and SD; N=5). Paired-pulse recovery ratio was calculated by taking the ratio of the amplitude of the second chemical IPSP (A_2) to the amplitude of the first chemical IPSP (A_1) (inset). Solid curves show single exponential decay fits to the recovery ratios. Arrows show the recovery of each synapse as the IPI tends to zero (R0). **C.** The recovery time constant τ_{rec} measured from exponential decay fits (as in panel B) plotted against D_{max} ($=1-R_0$) for each LP to PD (filled circles) and LP to PY synapse (open square). The LP to PD synapse has a faster time constant of recovery and smaller maximum depression than the LP to PY synapse.

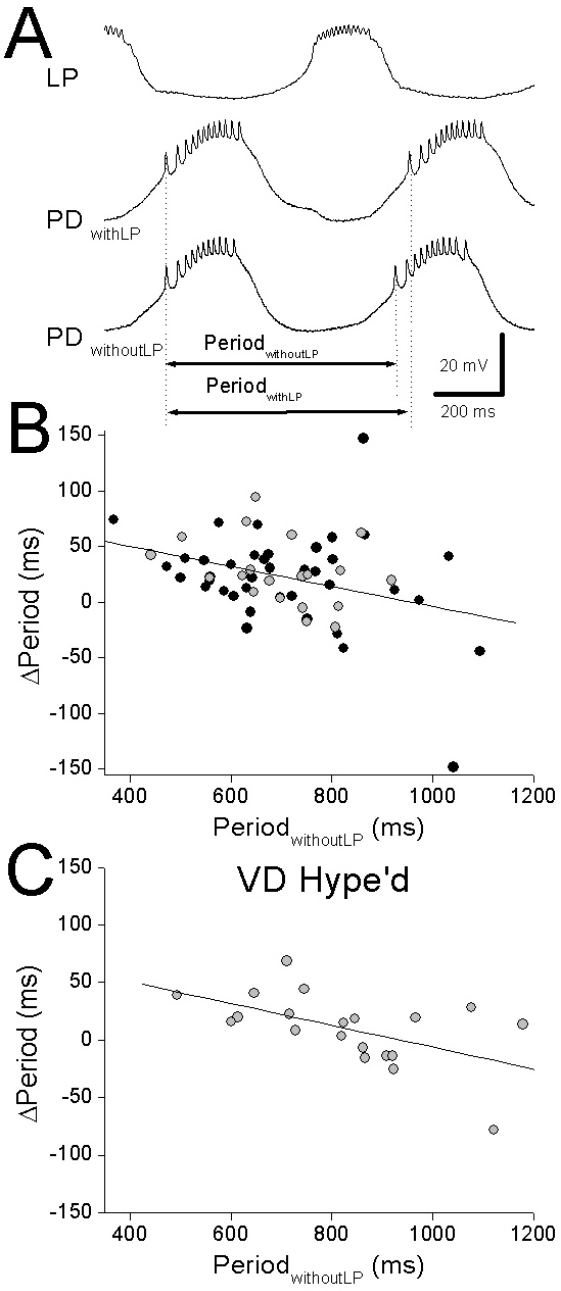

Figure 3. *The LP to PD synapse speeds up the rhythm when the period is short, but slows down the rhythm when it is long.* **A.** An example of intracellular voltage traces from the LP and PD neurons before and after hyperpolarization of the LP neuron. In this example, $Period_{withLP}$ was longer than $Period_{withoutLP}$. Thus, the LP to PD synapse increased the rhythm period. Minimum membrane potential values (in mV), LP: -62, PD_{withLP}: -66, $PD_{withoutLP}$: -62. **B.** Overall, ΔPeriod is negatively correlated with the $Period_{withoutLP}$. **C.** In a subset of the preparations (gray circles in panel B), the negative correlation between ΔPeriod and $Period_{withoutLP}$ was not statistically significant when the VD neuron was present, but became significant when the VD neuron was hyperpolarized. Lines in B and C show linear regression fits.

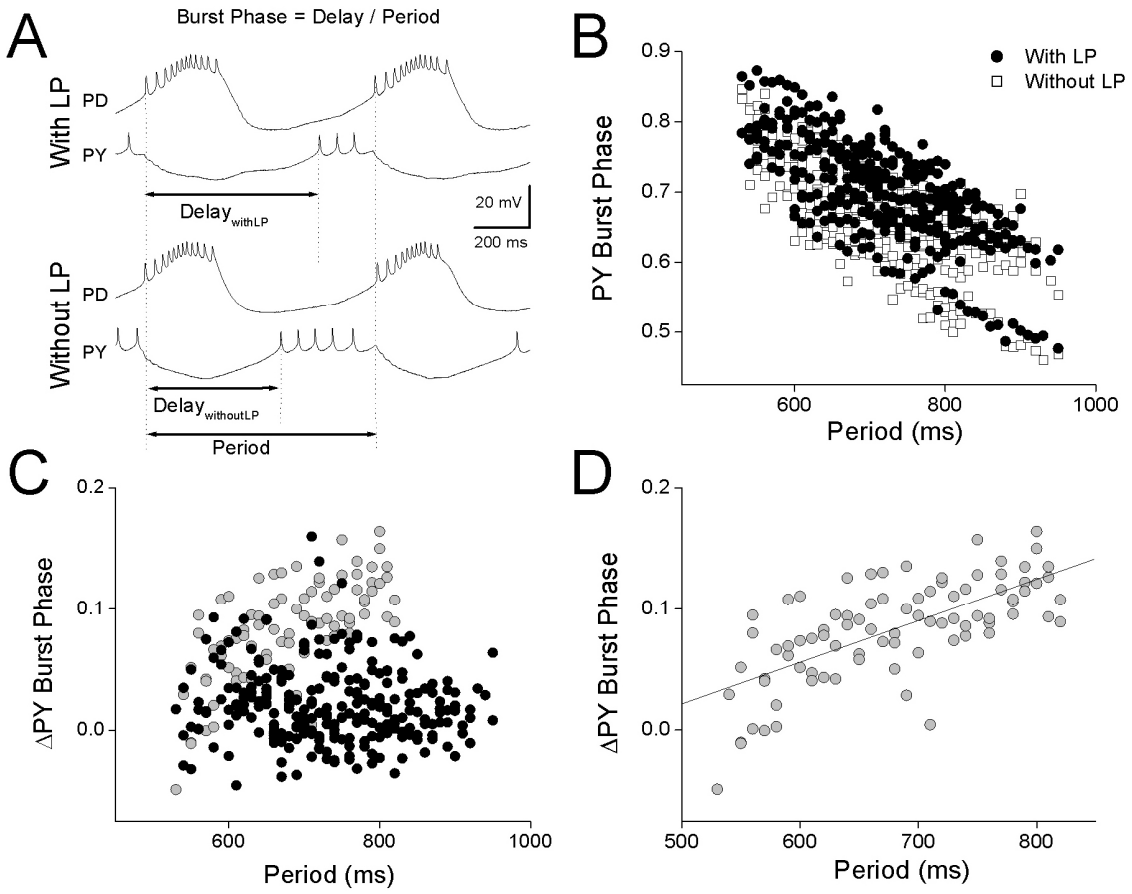

Figure 4. *The LP to PY synapse delays the burst phase of the PY neuron.* **A.** An example of intracellular voltage traces from the PD and PY neurons before and after hyperpolarization of the LP neuron. The burst phase of the PY neuron was calculated by dividing the time delay from onset of the PD burst to the onset of the PY burst by the PD neuron period. As seen in this example, the onset of the PY burst was delayed in the presence of the LP to PY synapse. Minimum membrane potential values (in mV), With LP, PD: -63, PY: -62; Without LP: PD: -59, PY: -62. **B.** PY burst phase with and without the LP to PY synapse plotted against the rhythm period. Overall, the LP to PY synapse delayed the burst phase of the PY neuron. **C.** The change in the PY burst phase (ΔPY) in the presence and absence of the LP neuron did not have a statistically significant correlation with the rhythm period. **D.** When analyzed separately, a subset of the preparations (gray circles in panel C) showed a significant positive correlation between the ΔPY burst phase and the rhythm period. Line shows linear regression fit.

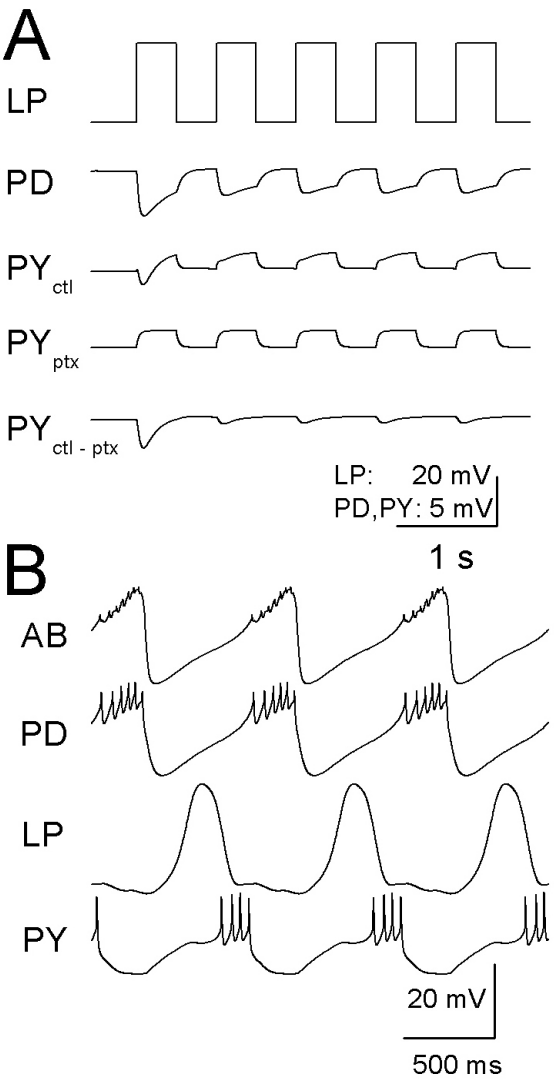

Figure 5. *The computational model fits the dynamics of the LP to PD and LP to PY synapses.* **A.** Voltage traces of the model PD and PY neurons in response to a train of 40 mV voltage pulses applied to the model LP neuron. For the PY neuron, traces when only the electrical component was present (ptx) and only the chemical component was present (ctl-ptx) are also shown. **B.** Voltage traces of the model AB, PD, and PY neurons producing rhythmic activity similar to the pyloric rhythm and the LP waveform used to activate the synapse.

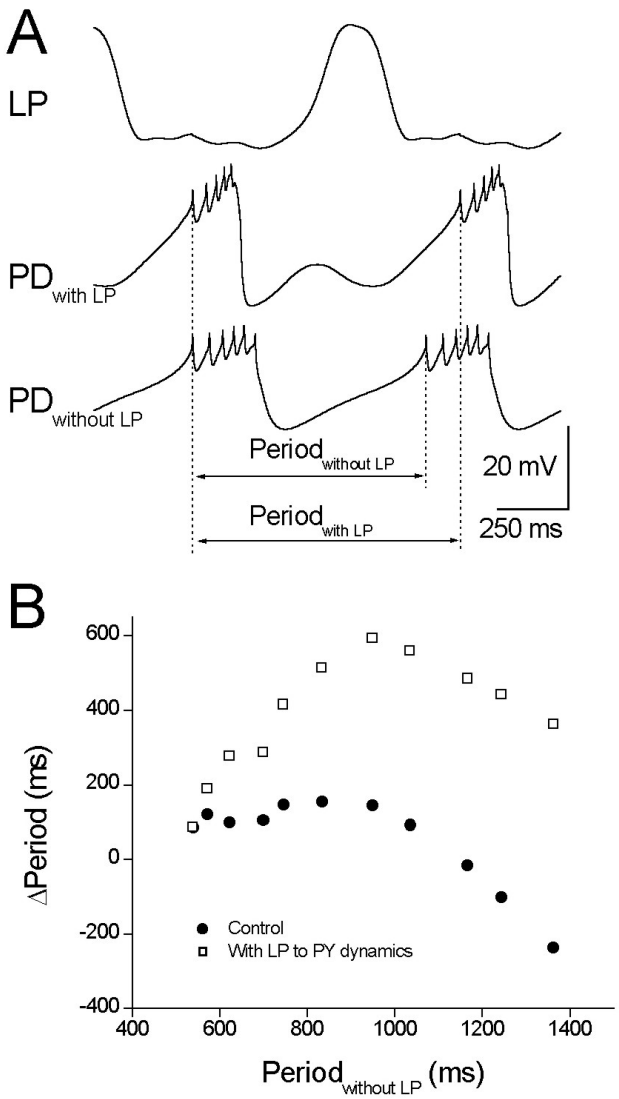

Figure 6. *The model LP to PD synapse fails to function properly when its short-term dynamics are replaced with those of the LP to PY synapse.* **A.** An example of voltage traces of the model LP neuron (top) and the model PD neuron with and without the model LP to PD synapse (the second trace and the third trace respectively). In this example, model LP to PD synapse increased the rhythm period. **B.** The ΔPeriod plotted against the $Period_{withoutLP}$ when the model LP to PD synapse has proper dynamics for the short-term depression (black circle), and when its dynamics for the short-term depression was replaced with those for the LP to PY synapse (square). The LP to PD synapse with the short-term depression of the LP to PY synapse failed to perform the proper function.

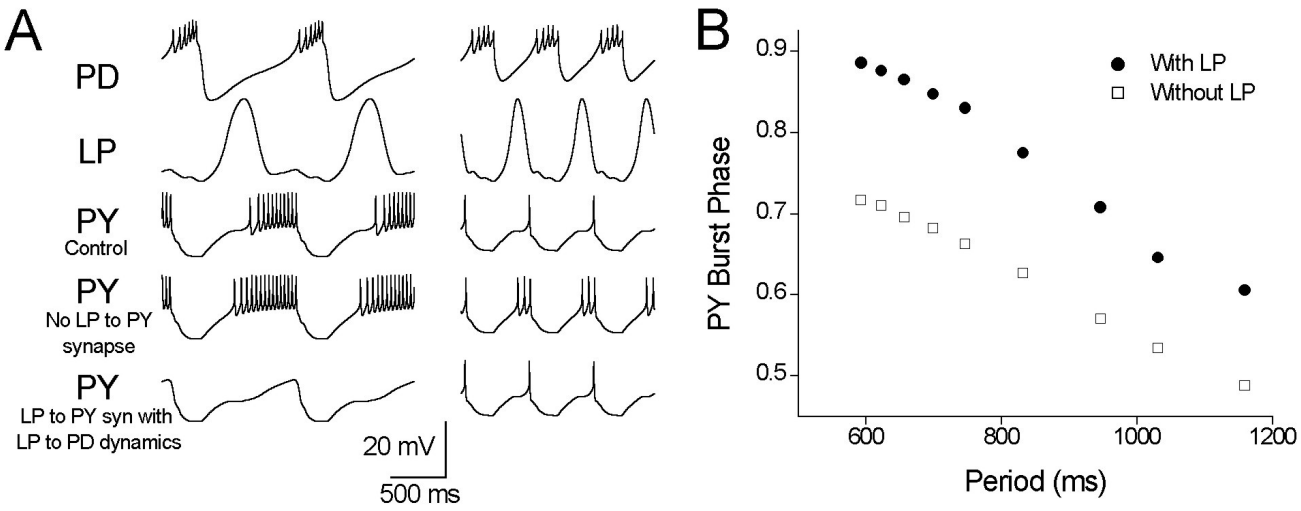

Figure 7. *The model LP to PY synapse fails to function properly when its short-term dynamics are replaced with those of the LP to PD synapse.* A. An example of voltage traces of the model PD, LP, and PY neurons when the rhythm period was long (left side) and short (right side). For the model PY neuron, traces with control LP to PY synapse (the third trace), without LP to PY synapse (the fourth trace), and with LP to PY synapse with the LP to PD dynamics (the bottom trace) are shown. When the dynamics of the LP to PY synapse were replaced with those for the LP to PD synapse, the PY neuron failed to fire an action potential at the long period. B. The PY burst phase with and without the LP to PY synapse plotted against the rhythm period.